

# A novel ISAR imaging algorithm for maneuvering target based on parameter estimation method

Hong-cai Xin\* and Bing-zhao Li†

\* Beijing Institute of Technology, Beijing, China

E-mail: hc\_xin\_bit@163.com Tel/Fax: +86-10-81384471

† Beijing Institute of Technology, Beijing, China

E-mail: li\_bingzhao@bit.edu.cn Tel/Fax: +86-10-81384471

**Abstract**—Traditional range-Doppler (RD) imaging methods for maneuvering targets have low resolution and poor capability of noise suppression. Range-instantaneous-Doppler (RID) attracts more and more attention in recent years. In this paper, a novel ISAR imaging method for maneuvering targets based on an effective parameter estimation method called the product form of the simplified linear canonical transform (SLCT) of symmetric correlation function (PSLSCF) is proposed, which can provide well-focus image of target. In the proposed method, the azimuth echo can be firstly modeled as multi-component cubic phase signal (CPS) after preprocessing, which leads to the time-varying Doppler frequency. After reducing phase order by a symmetric correlation function, SLCT is employed to estimate two parameters of CPS simultaneously with high accuracy and production form in SLCT domain is able to suppress cross term effectively. Finally, associated with RID imaging technology, a novel ISAR imaging algorithm is presented based on PSLSCF method. Moreover, computation burden is analyzed according to main procedure. The performances of PSLSCF method and the corresponding high-resolution ISAR imaging algorithm of target are verified respectively by numerical signal, simulated and real data.

**Index Terms**—Inverse synthetic aperture radar, simplified linear canonical transform, parameter estimation, high resolution

## I. INTRODUCTION

High-resolution inverse synthetic aperture radar (ISAR) imaging is a promising remote sensing technology and can be used in feature extraction, the target recognition, air/space surveillance and so on in all-weather conditions. It has received much attention of many researchers in the past decades [1], [2], [3], [4]. The conventional range-Doppler (RD) algorithm [5] fails to acquire well-focus image of target with complex motion, for which the Doppler is time-varying. To improve the resolution of image, range-instantaneous-Doppler (RID) imaging technology [1], [6], [7] has been presented and widely used in ISAR imaging system.

There are two categories according to the processing technique of echo signal: (1) non-parameter RID imaging technology, which can obtain ISAR image via time-frequency representation (TFR) [8], [9], [10]. Nevertheless, these TFRs bring a conflict between the resolution and cross-term suppression, which deteriorates the quality of ISAR image. (2) parametric RID technique dose not suffer from such problem brought by TFRs, in which azimuth echo signal can be modeled as appropriate polynomial phase signal (PPS) with

phase parameters. Recently, many researchers tend to model echo signal as the high-order phase signal, especially cubic phase signal (CPS). So far several successful ISAR imaging algorithms for CPS [3], [7], [12], [11], [13], [14], [15]. have been presented and generally listed into two categories: non-correlation algorithms like [11] require three-dimensional searching, which leads to high computational cost inevitably. In addition, several representative correlation algorithms have been proposed. However, ISAR imaging method based on the product high-order matched-phase transform (PHMT)[12] estimate parameter one by one, which results in error propagation. Modified Lv's distribution (MLVD) [13] fails to distinguish two signal when they are close in time-frequency domain, which can not achieve better resolution. Coherently integrated generalized cubic phase function (CIGCPF) and coherently integrated cubic phase function (CICPF) in [14] need to design an appropriate phase-terms function to improve the suppression ability of the cross term. The product form of symmetric correlation function based on the fractional Fourier transform (PFrSCF) in [15] works well in ISAR imaging but with high computational cost respectively.

In order to solve above problems and estimate parameters of CPS accurately, the simplified linear canonical transform (SLCT) [16] is taken a fancy to estimate parameters of CPS. SLCT is also a generalization of Fourier transform, which has the characteristics of simple implementation and lower computational complexity than FRFT[16], [17]. In this paper, a novel parameter estimation method called the product form of SLCT of symmetric correlation function (PSLSCF) is proposed. Firstly, LFM signal is obtained via symmetric correlation function (SCF). Then SLCT is employed to estimate two parameters simultaneously with high accuracy. In order to suppress cross terms effectively, product operation in SLCT domain can be adopted. So far parameter estimation method (PSLSCF) is reproduced. Subsequently, we present a novel ISAR imaging algorithm based on PSLSCF method and its computation cost is discussed in detailed. Numerical simulation of signals are tested to verify good ability of proposed PSLSCF method compared with CIGCPF and MLVD method in terms of parameter estimation and cross term suppression. Experiments with simulated data and real data further validate superior performance of proposed ISAR imaging algorithm compared with RD technique.

This paper is organized as follows. In Section II, the model of echo signal is given for target with complex motion and SLCT is introduced. Section III presents the parameter estimation method PLSLSCF in detail and high resolution ISAR imaging algorithm based on PLSLSCF. The better parameter estimation ability of PLSLSCF is verified by numerical signal and superior imaging performance is evaluated by simulated data and real data of target in Section IV. Section V is conclusion.

## II. PRELIMINARY

### A. Signal Model

Suppose transmitted signal is LFM signal, the received echo has been processed via range compression and motion compensation. Then the azimuth echo of the scatterer  $P$  is expressed as follows

$$\begin{aligned} s_p(t) &= A_p \exp \left[ -j \frac{4\pi}{\lambda} R(t) \right] \\ &= A_p \exp \{ j2\pi (a_0 + a_1 t + a_2 t^2 + a_3 t^3) \} \end{aligned} \quad (1)$$

where  $t \in [-T_a/2, T_a/2]$ ,  $R(t)$  is time-varying range from scatterer and radar,  $\lambda$  denotes wave length of transmitted signal.  $A_p$  is the amplitude,  $a_0, a_1, a_2$ , and  $a_3$  are the initial phase, center frequency, chirp rate, and rate of chirp rate, respectively. Then we can obtain the mathematical model of echo signal from all scatterers in a range cell, namely multi-component CPS as follows

$$s(t) = \sum_{i=1}^K A_i \exp \{ j2\pi (a_{i1} t + a_{i2} t^2 + a_{i3} t^3) \} \quad (2)$$

where  $A_i$  is amplitude of the  $i$ th echo signal,  $a_{i1}, a_{i2}, a_{i3}$  are the phase coefficients to be estimated.

In the practical environment,  $K$  is generally unknown, and one can employ the residual energy error to determine the number  $K$  of component. Note that it does not matter to omit the constant, because it does not affect the imaging result.

### B. Simplified Linear Canonical Transform

The linear canonical transform (LCT) [18], [19] with real parameter matrix  $A$  of signal  $x(t)$  is defined as

$$L_x^A(u) = \int_{-\infty}^{+\infty} x(t) K_A(t, u) dt \quad (3)$$

with the kernel

$$K_\alpha(u, t) = \begin{cases} \frac{1}{\sqrt{j\alpha}} \exp \{ j\pi (at^2 + du^2 - 2tu)/\alpha \}, & \alpha \neq 0 \\ \sqrt{d} \exp \{ j\pi (cdu^2)/2 \} \delta(t - du), & \alpha = 0 \end{cases} \quad (4)$$

where the real parameter matrix  $A = \begin{bmatrix} a & b \\ c & d \end{bmatrix}$  and  $|A| = ad - bc = 1$ .

If the parameter matrix  $A$  is chosen as a special matrix  $A = \begin{bmatrix} \cot \alpha & 1 \\ -1 & 0 \end{bmatrix}$ , then LCT reduces to a special transform with

parameter  $\alpha$ , namely

$$\begin{aligned} L_x^\alpha(u) &= \sqrt{j} \cdot L_x^A(u) = \int_{-\infty}^{+\infty} x(t) \exp \{ j\pi \cot \alpha t^2 - j2\pi t u \} dt, \\ &\alpha \in [0, \pi] \end{aligned} \quad (5)$$

When  $x(t)$  is a LFM signal with  $t \in [-\frac{T}{2}, \frac{T}{2}]$ ,

$$x(t) = \exp \left\{ j2\pi \left( f_0 t + \frac{1}{2} \gamma t^2 \right) \right\} \quad (6)$$

SLCT is able to gather the energy of signal and obtain acquire the center frequency and chirp rate when  $\cot \alpha = -\gamma$

$$\begin{aligned} L_x^\alpha(u) &= \int_{-\frac{T}{2}}^{\frac{T}{2}} x(t) \cdot \exp \{ j\pi (\cot \alpha t^2 - 2tu) \} dt \\ &= \int_{-\frac{T}{2}}^{\frac{T}{2}} \exp \{ j\pi (\cot \alpha + \gamma) t^2 \} \exp \{ -j2\pi (u - f_0) t \} dt \\ &= T \text{sinc} [T(u - f_0)] \end{aligned} \quad (7)$$

where  $\text{sinc}(t) = \frac{\text{sinc}(\pi t)}{\pi t}$ ,  $u$  is the frequency in SLCT domain.

From (7), therefore, the position of peak is determined by  $\alpha$  and  $u$ . We can estimate two parameters simultaneously by the SLCT as follows

$$\begin{cases} [\alpha_0, u_0] = \arg \max_{\alpha, u} \{ L_x^\alpha(u) \} \\ \hat{\gamma} = -\cot \alpha \\ \hat{f}_0 = u_0 \end{cases} \quad (8)$$

where  $\alpha \in [0, \pi]$ ,  $\hat{\gamma}$  and  $\hat{f}_0$  are the estimated chirp rate and center frequency respectively.

## III. MAIN METHOD

### A. Proposed PLSLSCF Method

Without loss of the generality, we discuss the two-component CPS

$$\begin{aligned} s(t) &= \sum_{i=1}^2 A_i \exp \{ j2\pi (a_{i1} t + a_{i2} t^2 + a_{i3} t^3) \} \\ &t \in [-T_a/2, T_a/2] \end{aligned} \quad (9)$$

In order to reduce phase order of (9), a symmetric correlation function  $SCF(t, \tau)$  of the signal  $s(t)$  is employed

$$\begin{aligned} SCF(t, \tau) &= s(t + \tau) s^*(t - \tau) \\ &\cdot [s(t + \tau + \tau_0) s^*(t - \tau - \tau_0)]^* \\ &= SCF_{\text{auto}}(t, \tau) + SCF_{\text{cross}}(t, \tau) \end{aligned} \quad (10)$$

where the auto term is shown in (11) with  $\phi_i(\tau) = \exp \{ -j2\pi (2a_{i1} \tau_0 + 2a_{i3} \tau_0^3) \} \exp \{ -j2\pi (6a_{i3} \tau_0^2 \tau + 6a_{i3} \tau_0 \tau^2) \}$ . And  $SCF_{\text{cross}}(t, \tau)$  denotes the cross term, which is not given unnecessary details here and the range of  $\tau$  can be deduced can be referred to [15].

*Remark 1: It should be noted that the choice of  $\tau_0$ . Large  $\tau_0$  would generate the spectrum ambiguity. Selecting a proper fixed lag time  $\tau_0$  can avoid the spectrum problem and ensure the estimation accuracy as far as possible. We give the result as*

$$\begin{aligned}
 SCF_{auto}(t, \tau) &= \sum_{i=1}^2 A_i^4 \exp\{-j2\pi(2a_{i1}\tau_0 + 2a_{i3}\tau_0^3)\} \cdot \exp\{-j2\pi(6a_{i3}\tau_0^2\tau + 6a_{i3}\tau_0\tau^2)\} \\
 &\quad \cdot \exp\{-j2\pi(4a_{i2}\tau_0t + 6a_{i3}\tau_0t^2)\} \\
 &= \sum_{i=1}^2 A_i^4 \phi_i(\tau) \cdot \exp\{-j2\pi(4a_{i2}\tau_0t + 6a_{i3}\tau_0t^2)\}
 \end{aligned} \tag{11}$$

follows

$$\tau_0 \leq \frac{T_a}{4} \tag{12}$$

We therefore choose  $\tau_0 = T_a/8$  in this paper, which is analyzed in [15].

The SLCT of  $SCF(t, \tau)$  along with  $t$  axis is shown as follows

$$\begin{aligned}
 SLSCF(u, \tau) &= \int_{-T_a/2}^{T_a/2} SCF(t, \tau) K_A(t, u) dt \\
 &= SLSCF_{auto}(u, \tau) + SLSCF_{cross}(u, \tau)
 \end{aligned} \tag{13}$$

$SLSCF_{auto}(u, \tau)$  and  $SLSCF_{cross}(u, \tau)$  denote the auto terms and cross terms generated by (10) via SLCT. When  $\cot \alpha_i = 12a_{i3}\tau_0$

$$\begin{aligned}
 SLSCF_{auto}(u, \tau) &= \int_{-T_a/2}^{T_a/2} SCF_{auto}(t, \tau) K(u, t) dt \\
 &= \sum_{i=1}^2 T_a A_i^4 \phi_i(\tau) \cdot \text{sinc}[T_a(u + 4a_{i2}\tau_0)]
 \end{aligned} \tag{14}$$

From (14), it is easy to find that the energy of auto terms can be gathered to be peaks independent of  $\tau$ . In fact, cross terms do not share this property and the specific analysis can be referred to [15]. Hence, in order to suppress the cross term of multi-component CPS, we can product  $PSLSCF(u, \tau)$  in SLCT domain by choosing  $\tau$  at different time, i.e.,

$$PSLSCF(u) = \prod_{l=1}^L SLSCF(u, \tau_l) \tag{15}$$

where  $L$  is the number of chosen  $\tau$ .

*Remark 2:* The size of  $L$  determines performance in terms of the cross term suppression and computational cost. If  $L$  is too small, it is so difficult to suppress effectively, and if too large, it bears more computational burden. For the balance of them, we choose  $L = 15$ .

### B. Proposed ISAR Imaging Algorithm Based on PSLSCF

In this Subsection, a novel ISAR imaging algorithm based on PSLSCF can be presented. Fig. 1 is the flowchart of proposed ISAR imaging algorithm. The implementation procedure is illustrated in detail as follows.

*Step. 1:* Perform the range compression by dechirp technique and the motion compensation to the radar echo data.

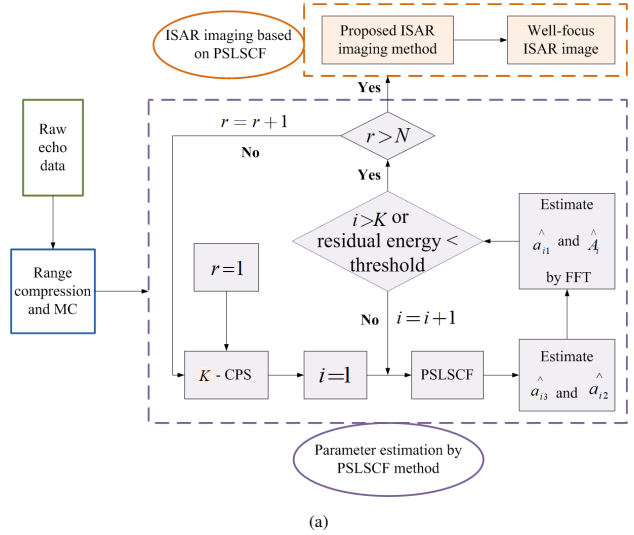


Fig. 1. The flowchart of proposed ISAR imaging algorithm

*Step. 2:* Model the received signal in  $r$ th range bin as

$$s(t) = \sum_{i=1}^K A_i \exp[j2\pi(a_{i1}t + a_{i2}t^2 + a_{i3}t^3)] \tag{16}$$

where  $K$  is the component number of the CPS in the  $r$ th range bin,  $A_i$  denotes the amplitude and  $a_{i1}, a_{i2}, a_{i3}$  are the coefficients of the  $i$ th component, respectively.

*Step. 3:* Initialize  $i = 1$ ,

$$s_i(t) = A_i \exp\{j2\pi(a_{i1}t + a_{i2}t^2 + a_{i3}t^3)\} \tag{17}$$

*Step. 4:* Apply the PSLSCF method to  $s_i(t)$ , then parameters  $\hat{a}_{i3}$  and  $\hat{a}_{i2}$  can be obtained simultaneously.

*Step. 5:* Construct the compensation function according to estimation parameters in *Step. 4*

$$s_{com}(t) = \exp\{-j2\pi(\hat{a}_{i2}t^2 + \hat{a}_{i3}t^3)\} \tag{18}$$

and obtain the sinusoid signal with parameter  $\hat{a}_{i1}$

$$s_{sin} = s(t) \cdot s_{com}(t). \tag{19}$$

*Step. 6:* Apply the FFT to  $s_{sin}$  to obtain  $\hat{a}_{i1}$  and then the

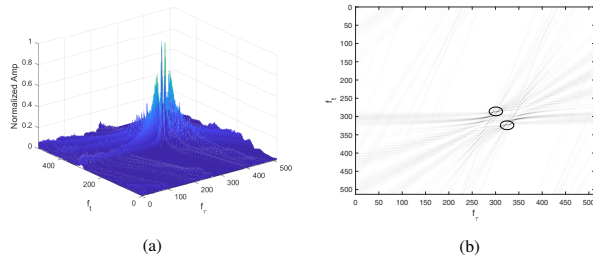


Fig. 2. The result for two closed signal by CIGCPF. (a) 3-D result (b) the grayscalemap

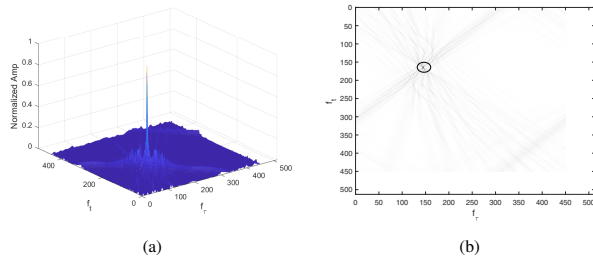


Fig. 3. The result for two closed signal by MLVD. (a) 3-D result (b) the grayscalemap

amplitude  $\hat{A}_i$  obtained by

$$\hat{A}_i = \frac{1}{N} \left| \sum_{-N/2}^{N/2-1} s_i(t) \cdot \exp\{-j2\pi(a_{i1}t + a_{i2}t^2 + a_{i3}t^3)\} \right| \quad (20)$$

where  $t = n \cdot \Delta t$ ,  $n = -N/2, \dots, N/2 - 1$  and  $\Delta t$  is the sample interval.

Step. 7: Reconstruct the  $i$ th component of CPS by the estimated parameters

$$s_i(t) = \hat{A}_i \cdot \exp\{-j2\pi(a_{i1}t + a_{i2}t^2 + a_{i3}t^3)\}, \quad (21)$$

and then subtract it from  $s(t)$  by the notch filter with proper center and bandwidth.

Step. 8: Let  $i = i + 1$  and repeat Step. 3–7 until  $i = K$ . If the  $K$  is unknown, repeat Step 3-7, and then end up until that the residual energy is less than a fixed threshold in the  $r$ th range bin.

Step. 9: Let  $r = r + 1$  and repeat Step. 2–8 until  $r = N$ .

Step. 10: The well-focused ISAR image can be obtained.

### C. Computation Cost

In proposed method, it is necessary to analyze the computation cost, which is composed of the main procedure. For

TABLE I  
PARAMETERS OF SIGNAL

parameter	$A$	$a_{i1}$	$a_{i2}$	$a_{i3}$
$s_1(t)$	1	1/64	1/5N	1/10N <sup>2</sup>
$s_2(t)$	1	1/32	3/20N	1/5N <sup>2</sup>

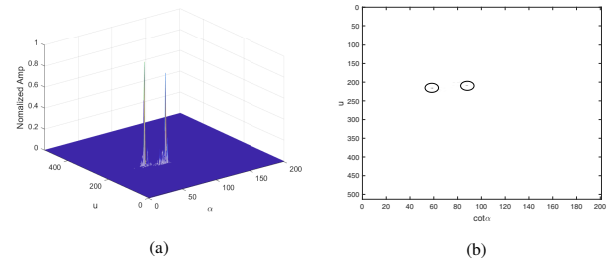


Fig. 4. The result for two closed signal by PSLCPF. (a) 3-D result (b) the grayscalemap

received echo signal matrix with  $N$  range bins and  $M$  Doppler bins, (1) SCF:  $4M \cdot N$ ; (2) PSLSCF:  $L \cdot N \cdot M \log_2 M$ ; (3) FFT:  $N \cdot M \log_2 M$ . Thus, the computation cost can be calculated to be  $4MN + (L + 1)NM \log_2 M$ .

## IV. SIMULATION

### A. Numerical Signal

In order to testify the effectiveness of proposed PSLSCF method for parameter estimation, two-component CPS is used and phase parameter is shown in TABLE I. Different estimation methods are compared including CIGCPF and MLVD. The auto terms in Fig. 2(b) to Fig. 4(b) are marked by black circle. From Fig. 2, it has some trouble to separate two signal for CIGCPF method and cross-term distracts the result seriously. Moreover, Although the result by MLVD method in Fig. 3 is able to suppress cross-term, it can not detect two different signal and only shows one of the two-component signal, for which it just distribute the one time-frequency domain. However, Fig. 4 works very well in detect signal and cross-term suppression, which is the result by our proposed method in different time-frequency domains. Thus, we conclude that our proposed method is able to estimate parameter accurately and suppress cross-term with superior performance, which helps people to acquire high-quality images. There is no need to proof the fact that, thus, the proposed ISAR imaging algorithm based on PSLSCF is bound to lead to better imaging capacity in the next two Subsection.

### B. ISAR Imaging Based on Simulated Data

In this Subsection, we use the simulated data to evaluate the proposed ISAR imaging algorithm. The parameters of radar are shown in TABLE II. The initial range from radar to target is assumed as 10 km and target is with size 100 m. For complex motion, the parameters are supposed that velocity of rotation is 0.01 rad/s, acceleration of rotation and acceleration rate of rotation are 0.08 rad/s<sup>2</sup> and 0.03 rad/s<sup>3</sup> respectively. Here white Gaussian noise is embedded into the echo signals and SNR is -1 dB. Fig. 5(a) is a simple ship target model and the traditional RD image is shown in Fig. 5(b), which is blurred severely. In order to validate our proposed method, the ISAR imaging results different moments are tested, which are shown Fig. 6(a) and Fig. 6(b). Compared Fig. 6 with Fig. 5(b), we can find Fig. 6 with higher resolution is clear, which

TABLE II  
THE PARAMETER OF RADAR AND TARGET

parameter	value
center frequency (GHz)	10
bandwidth (MHz)	150
PRF (Hz)	500
pulse length ( $\mu s$ )	0.5
range bin number	400
pulse number	400

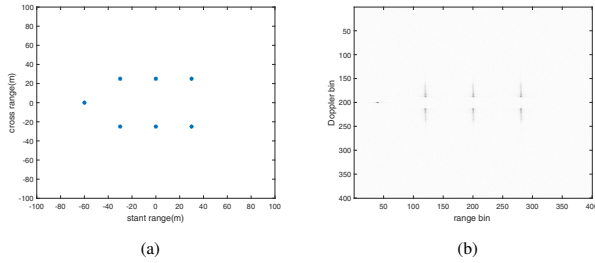


Fig. 5. ISAR images (a) the target (b) RD image

do not defocus comparatively. Entropy can be calculated and shown in TABLE III. It can be proved further the fact that our proposed method is more suitable for target with complex motion according smaller entropy, which is resulted by high accuracy of proposed PSLSCF method.

TABLE III  
ENTROPY OF IMAGE FOR SIMULATED DATA

RD	PSLSCF	
	$t = 0.110s$	$t = 0.222s$
11.76	4.260	3.9174

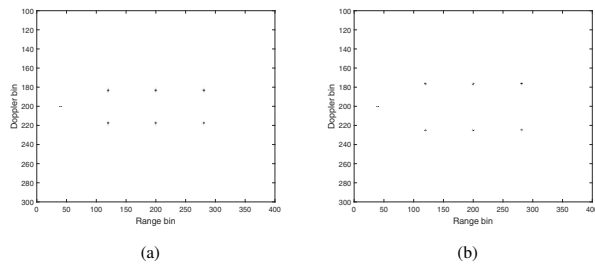


Fig. 6. ISAR images based on the PSLSCF algorithm: (a)  $t = 0.116s$  (b)  $t = 0.222s$

C. ISAR Imaging Based on Real Data

In this Subsection, the real data can be used to validate the performance of proposed ISAR imaging algorithm. TABLE V shows the parameters of radar. The ship target is with size  $24m$ , and velocity is  $8 m/s$ . The initial range from target to

TABLE IV  
ENTROPY OF IMAGE FOR REAL DATA

RD	PSLSCF	
	$t = 0.105s$	$t = 0.280s$
10.26	4.2219	4.3054

TABLE V  
THE PARAMETER OF RADAR AND TARGET

parameter	value
center frequency (GHz)	9.25
bandwidth (MHz)	500
PRF (Hz)	200
pulse length ( $\mu s$ )	600
range bin number	256
pulse number	256

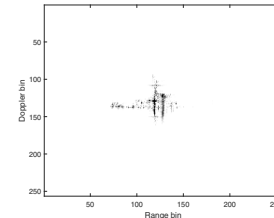


Fig. 7. RD image

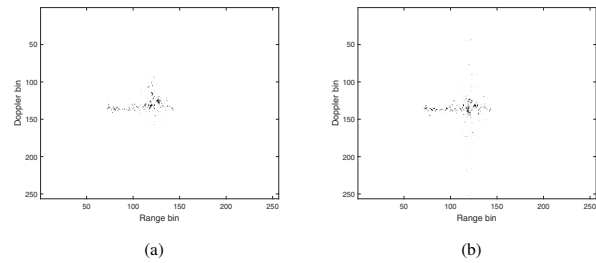


Fig. 8. ISAR images based on the PSLSCF algorithm. (a)  $t = 0.105s$  (b)  $t = 0.280s$

radar is  $6000 m$ . The RD image is also used to be compared and shown in Fig. 7. It can be found that Fig. 7 is obscured and low-resolution because many scatterers are not separated. Fig. 8 is the well-focus result by our proposed method and Fig. 8(a) and Fig. 8(b) are obtained at different moment  $t = 0.105s$  and  $t = 0.280s$  respectively. From TABLE IV, smaller entropy is obtained, which is benefit by good performance of proposed PSLSCF in the terms of parameter estimation.

V. CONCLUSION

This paper presents an ISAR imaging algorithm based on the proposed PSLSCF method. After range compression and motion compensation, for target with complex motion,

echo signal is modeled as multicomponent CPS firstly. Then proposed PSLSCF method is used to estimate phase parameters accurately and suppresses the cross term by production operation in SLCT domain effectively. Finally, associated with RID imaging technique, a novel ISAR imaging algorithm with high-resolution characteristic is presented. Numerical signal is used to verify the good ability of cross term suppression and parameter estimation. Superior performance of the proposed ISAR imaging algorithm based on PSLSCF method are validated by experiments with simulated data and real data at moderate computation cost.

#### ACKNOWLEDGMENT

This work was supported by the National Natural Science Foundation of China [No. 61671063] and China Scholarship Council.

#### REFERENCES

- [1] F. Berizzi, E. D. Mese, M. Diani, M. Martorella, "High-resolution ISAR imaging of maneuvering targets by means of the range instantaneous Doppler technique: Modeling and performance analysis", *IEEE Trans. Imag. Process.*, vol. 10, no. 12, pp. 1880-890, Dec. 2001
- [2] Y. Wang, Y. C. Jiang, "ISAR imaging of maneuvering target based on the L-class of fourth-order complex-lag PWVD", *IEEE Trans. Geosci. Remote Sens.*, vol. 48, no. 3 pp. 1518-1527, Mar. 2010
- [3] J. B. Zheng, W. T. Zhu, L. Zhang, Z. Liu, Q. H. Liu, "ISAR imaging of nonuniformly rotating target based on a fast parameter estimation algorithm of cubic phase signal", *IEEE Trans. Geosci. Remote Sens.*, vol. 53, no. 9, pp. 4727-4740, Sep. 2015
- [4] Y. X. Gao, Z. J. Zhang, L. Guo, "ISAR Imaging and Cross-Range Scaling for Maneuvering Targets by Using the NCS-NLS Algorithm", *IEEE Sensors J.*, vol. 19, no. 13, pp. 4889-4897, Jul. 2019
- [5] J. L. Walker, "Range-Doppler imaging of rotating objects", *IEEE Trans. Aerosp. Electron. Syst.*, vol. AES-16, no. 1, pp. 23-52, Jan. 1980
- [6] V. C. Chen, H. Ling, "Time-frequency Transform for Radar Imaging and Signal Analysis", Norwood, MA, USA, Artech House, 2002
- [7] X. Bai, R. Tao, Z. J. Wang, Y. Wang, "ISAR imaging of a ship target based on parameter estimation of multicomponent quadratic frequency modulated signals", *IEEE Trans. Geosci. Remote Sens.*, vol. 52, no. 2, pp. 1418-1429, Feb. 2014
- [8] Z. Bao, C. Sun, M. Xing, "Time-frequency approaches to ISAR imaging of maneuvering targets and their limitations", *IEEE Trans. Aerosp. Electron. Syst.*, vol. 37, no. 3, pp. 1091-1099, Jul. 2001
- [9] X. G. Xia, G. Wang, V. C. Chen, "Quantitative SNR analysis for ISAR imaging using joint time-frequency analysis-short time Fourier transform", *IEEE Trans. Aerosp. Electron. Syst.*, vol. 38, no. 2, pp. 649-659, Apr. 2002
- [10] M. D. Xing, R. Wu, Y. Li, Z. Bao, "New ISAR imaging algorithm based on modified Wigner-Ville distribution", *IET Radar Sonar Nav.*, vol. 3, no. 1, pp. 70-80, Feb. 2009
- [11] L. Wu, X. Z. Wei, D. G. Wang, H. Q. Wang, X. Li, "ISAR imaging of target with complex motion based on discrete chirp Fourier transform for cubic chirps", *IEEE Trans. Geosci. Remote Sens.*, vol. 50, no. 10, pp. 4201-4212, Oct. 2012
- [12] Y. Wang, Y. C. Jiang, "ISAR imaging of a ship target using product high-order matched-phase transform", *IEEE Geosci. Remote Sens. Lett.*, vol. 6, no. 4, pp. 658-661, Oct. 2009
- [13] Y. Y. Li, T. Su, J. B. Zheng, X. H. He, "ISAR imaging of target with complex motions based on modified Lv's distribution for cubic phase signal", *IEEE J. Sel. Topics in Appl. Earth Observ. Remote Sens.*, vol. 9, no. 12, pp. 5688-5702, Dec. 2016
- [14] D. Li, X. G. Gui, H. Q. Liu, J. Su, H. Xiong, "An ISAR imaging algorithm for maneuvering targets with low SNR based on parameter estimation of multicomponent quadratic FM signal and nonuniform FFT", *IEEE J. Sel. Topics in Appl. Earth Observ. Remote Sens.*, vol. 9, no. 12, pp. 5688-5702, Dec. 2016
- [15] H. C. Xin, X. Bai, Y. E. Song, B. Z. Li and R. Tao, "ISAR imaging of target with complex motion associated with the fractional Fourier transform", *Digit. Signal. Process.*, vol. 83, pp. 332-345, Oct. 2018
- [16] Y. Guo, L. D. Yang, "Method for parameter estimation of LFM signal and its application", *IET Signal Process.*, vol. 13, no. 5, pp. 538-543, Jun. 2019
- [17] S. H. Liu, T. Shan, R. Tao, Y. D. Zhang, G. Zhang, etc., "Sparse discrete fractional Fourier transform and its applications", *IEEE Trans. Signal Process.*, vol. 62, no. 24, pp. 6582-6595, Oct. 2014
- [18] Y. N. Zhang, B. Z. Li, " $\phi$ -linear canonical analytic signals", *Signal Process.*, vol. 143, pp. 181-190, Feb. 2018
- [19] Y. N. Sun, B. Z. Li, "Sliding discrete linear canonical transform", *IEEE Trans. Signal Process.*, vol. 66, no. 17, pp. 4553-4563, Sep. 2018
- [20] E. Sejdić, I. Djurović, L. Stanković, "Fractional Fourier transform as a signal processing tool: An overview of recent developments", *Signal Process.*, vol. 91, no. 6, pp. 1351-1369, Jun. 2011